Describing Dzyaloshinskii-Moriya spirals from first principles

M. Heide, G. Bihlmayer, and S. Blügel

Institut für Festkörperforschung and Institute for Advanced Simulation, Forschungszentrum Jülich, 52425 Jülich, Germany

Abstract

In magnetic systems lacking spatial inversion symmetry it is observed that the Dzyaloshinskii-Moriya interaction can entail long-ranged spin spirals with a unique sense of rotation. Here, we present a computationally efficient scheme to calculate these large magnetic structures within density functional theory and extract the interaction parameters using perturbative approaches of different order. We analyze the accuracy of these methods by investigating thin Fe films on W(110) and Mo(110) substrates.

Key words: Spiral spin-density waves, Dzyaloshinskii-Moriya interaction, first-principles calculations
PACS: 71.15.Mb, 71.15.Rf, 75.30.Fv, 75.70.Ak

1. Introduction

For the prediction and understanding of magnetic structures from first-principles calculations, a systematic investigation of magnetic interactions like exchange or the magnetocrystalline anisotropy (MCA) is crucial. The determination of the MCA requires relativistic (often collinear) total energy calculations. Exchange interactions can be extracted from energy differences between different magnetic structures. Here, the calculation of spiral spin-density waves (SSDWs) turned out to be an efficient approach since (i) SSDWs are solutions of the classical Heisenberg model and (ii) the generalized Bloch theorem can be exploited in the calculations [1,2].

Unfortunately, in this procedure a type of magnetic interactions is completely missed: the antisymmetric exchange or Dzyaloshinskii-Moriya (DM) interaction. In the past few years we have shown the particular importance of this interaction for magnetic nanostructures, e.g. ultrathin films on surfaces, where it can give rise to cycloidal SSDWs with a unique sense of rotation [3,4]. These SSDWs are induced by a relativistic effect (spin-orbit coupling, SOC) in inversion-asymmetric structures and typically have a long spatial period. Since SOC and the use of the generalized Bloch theorem are mutually exclusive, the relativistic description of these spin spirals requires noncollinear calculations on the basis of huge magnetic unit cells. As the performance of these calculation with sufficient accuracy is a true challenge, we present here a scheme which reduces the computational costs of such calculations drastically. Furthermore, we analyze the effect of the involved approximations and indicate how this scheme can be used for a detailed analysis of the results.

2. Ansatz

If the magnetic structure spatially varies on the mesoscopic scale, it can be described with a micromagnetic model where the atoms' magnetic moments are replaced by a continuous function $\mathbf{M}(\mathbf{r})$. The energy is a functional, $E[\mathbf{M}(\mathbf{r})]$, containing the magnetic interactions mentioned above. When the magnetization direction is confined to a plane and varies only along one spatial direction r, we describe the magnetization by a function of a single angle $\varphi(r)$ and the energy functional has the form [5,6]

$$E[\varphi] = \int \mathrm{d}r \left[A \left(\frac{\mathrm{d}\,\varphi}{\mathrm{d}\,r} \right)^2 + D \frac{\mathrm{d}\,\varphi}{\mathrm{d}\,r} + K(\varphi) \right] . \qquad (1)$$

Here, the spin stiffness A depends mainly on the non-relativistic exchange interactions, whereas the parameter D, induced by the DM-interaction, and the MCA term K are due to the spin-orbit coupling. In the following, we present a method to calculate the parameters of this energy functional from first principles.

In order to obtain the model parameters A and D by density functional theory (DFT), we calculate homogeneous SSDWs (i.e. spatially rotating magnetic structures with $\frac{\mathrm{d}\,\varphi}{\mathrm{d}\,r} = \text{const.}$) with different spatial period lengths $\lambda = 2\,\pi\,(\frac{\mathrm{d}\,\varphi}{\mathrm{d}\,r})^{-1}$. Then, Eq. (1) yields

$$E(\lambda) = A\Big(\frac{2\,\pi}{\lambda}\Big)^2 + D\,\frac{2\,\pi}{\lambda} + \bar{K} \tag{2}$$

with an anisotropy energy $\bar{K}$ averaged over the pitch of the spiral. A and D can be obtained from quadratic and linear fits to the dispersion curve $E(\lambda^{-1})$ in Eq. (2). It can be useful to split this curve into an even and an odd part before performing the linear fit, as the odd (linear) term typically is very small, whereas the even part can require higher numerical cutoffs for the same accuracy.

Of course, the method can also be applied for more than one spatial extension and general magnetization directions: From calculations of homogeneous SSDWs with different spatial propagation directions and different spin-rotation axes, all components of the vector $\mathbf{D}$, that describes the DM-interaction [7], can be obtained. One should keep in mind, that our approach is useful to obtain the exchange parameters of Eq. (1) but cannot be used to determine the magnetic structure directly from the electronic-structure calculations: The true Dzyaloshinskii spirals (that minimize the functional (1)) are not homogeneous [5,6], whereas our method relies on homogeneity. Nevertheless, with the parameters obtained by this method one can describe more complex magnetic states such as inhomogeneous SSDWs in the context of a micromagnetic model. This approach has been used successfully to describe e.g. domain walls [8].

3. Electronic structure of spin spirals

If spin-space and crystal lattice are not coupled, we can apply a generalized Bloch theorem that allows us to describe any homogeneous SSDW by using the chemical unit cell (instead of the magnetic one). Since spin-orbit coupling distinguishes between different magnetization directions with respect to the lattice in the chemical unit cells that make up the magnetic unit cell, using the generalized Bloch theorem is no longer possible and the computational expenses can increase dramatically. To circumvent this problem we exploit the fact that SOC is usually a weak effect and can be included in a perturbative way: First we neglect spin-orbit coupling and calculate the homogeneous SSDWs within one chemical unit cell and periodic boundary conditions, and then the action of the spin-orbit operator on these solutions will be considered in a second step.

3.1. *Generalized Bloch theorem*

Introducing spherical coordinates for the magnetization, $\mathbf{m}$, and the exchange-correlation $\mathbf{B}$-field,

$$\mathbf{m} = m\,(\sin\vartheta\,\cos\varphi\,\hat{\mathbf{e}}_x + \sin\vartheta\,\sin\varphi\,\hat{\mathbf{e}}_y + \cos\vartheta\,\hat{\mathbf{e}}_z)\;,$$

$$\mathbf{B} = B\,(\sin\vartheta\,\cos\varphi\,\hat{\mathbf{e}}_x + \sin\vartheta\,\sin\varphi\,\hat{\mathbf{e}}_y + \cos\vartheta\,\hat{\mathbf{e}}_z)\;,$$

we can characterize the homogeneous SSDW underlying Eq. (2) by

$$\begin{aligned} m(\mathbf{r}+\mathbf{R}) &= m(\mathbf{r})\;, \quad B(\mathbf{r}+\mathbf{R}) = B(\mathbf{r})\;, \\ \vartheta\,(\mathbf{r}+\mathbf{R}) &= \vartheta(\mathbf{r})\;, \quad \varphi(\mathbf{r}+\mathbf{R}) = \varphi(\mathbf{r}) + \mathbf{q}\cdot\mathbf{R}\;. \end{aligned} \tag{3}$$

Here, $\mathbf{R}$ is a lattice vector of the chemical lattice and the $\mathbf{q}$-vector determines the direction of spatial propagation of the SSDW as well as the period length $|\lambda| = \frac{2\,\pi}{|\mathbf{q}|}$. The spiral's rotational direction depends on the sign of $\mathbf{q}$.

The generalized Bloch theorem [1,2] states, that the eigenstates of a Schrödinger-type Hamiltonian

$$\mathcal{H}_0 = \frac{1}{2\,m_e}\,\mathbf{p}^2 + V(\mathbf{r}) + \boldsymbol{\sigma}\cdot\mathbf{B}(\mathbf{r}) \tag{4}$$

with a lattice periodic scalar potential V and a spiraling $\mathbf{B}$-field as given in Eq. (3) can be written in the form

$$\psi_{\mathbf{k},j}(\mathbf{r}|\mathbf{q}) = \begin{pmatrix} \psi^{(\uparrow)}_{\mathbf{k},j} \\ \psi^{(\downarrow)}_{\mathbf{k},j} \end{pmatrix} = \begin{pmatrix} e^{i\,(\mathbf{k}-\frac{1}{2}\mathbf{q})\cdot\mathbf{r}}\,u^{(\uparrow)}_{\mathbf{k},j}(\mathbf{r}) \\ e^{i\,(\mathbf{k}+\frac{1}{2}\mathbf{q})\cdot\mathbf{r}}\,u^{(\downarrow)}_{\mathbf{k},j}(\mathbf{r}) \end{pmatrix} \tag{5}$$

with lattice-periodic functions $u^{(\sigma)}_{\mathbf{k},j}(\mathbf{r}) = u^{(\sigma)}_{\mathbf{k},j}(\mathbf{r}+\mathbf{R})$. The $\mathbf{q}$-dependent phase factor, that is not present in the ordinary Bloch theorem, corresponds to a spin rotation around the z-axis. This theorem allows to determine the full solution of the Kohn-Sham Schrödinger equation by restricting the calculation to the chemical unit cell and the first Brillouin zone.

3.2. *Spin-orbit operator and force theorem*

After determining the selfconsistent solution of the Kohn-Sham Schrödinger equation with spiral boundary conditions, the spin-orbit coupling operator $\mathcal{H}_{\mathrm{so}}$ is added. This operator can be approximated [9,10] by a sum over individual atoms, μ,

$$\tilde{\mathcal{H}}_{\mathrm{so}} = \sum_{\mu}\,\xi^{(\mu)}(r^{(\mu)})\;\boldsymbol{\sigma}\cdot\mathbf{L}^{(\mu)}\;, \tag{6}$$

where $\mathbf{L}^{(\mu)}$ is the orbital momentum operator with respect to the position of the μth nucleus and $\xi^{(\mu)}(r^{(\mu)})$ describes the spin-orbit coupling strength as a function of the distance $r^{(\mu)}$ from the μth nucleus [11].

Note, that Eq. (3) implies a spin rotation axis parallel to $\hat{\mathbf{e}}_z$. As long as SOC was neglected, this did not restrict the generality of our approach, but at this point we might want to include a different direction of this axis. Then, the functions of Eq. (5) have to be rotated with a spin rotation matrix U or, equivalently, we assume that a rotated spin-orbit operator, $\mathcal{H}_{\mathrm{so}} = \mathsf{U}^{\dagger}\,\tilde{\mathcal{H}}_{\mathrm{so}}\,\mathsf{U}$, is used.

For the Hamiltonian $\mathcal{H}_0 + \mathcal{H}_{\mathrm{so}}$, we exploit the fact that SOC is a relatively small effect and can be treated as a perturbation. We use Andersen's force theorem [12–14], where the change of the total electronic energy due to a small perturbation is considered in a density functional theory context. In our case, we can apply it to the known selfconsistent solution of the unperturbed Kohn-Sham equation

$$\mathcal{H}_0[n_0, \mathbf{m}_0]\ \psi_{0,\nu} = \epsilon_{0,\nu}\ \psi_{0,\nu} \tag{7}$$

and the corresponding total energy E_0: According to the force theorem, the total energy E in presence of the perturbation can be approximated by

$$E - E_0 \approx \sum_{\nu}^{\mathrm{occ.}} \epsilon_{\mathrm{ft},\nu} - \sum_{\nu}^{\mathrm{occ.}} \epsilon_{0,\nu}\ . \tag{8}$$

Thereby, $\{\epsilon_{\mathrm{ft},\nu}\}$ represents the spectrum of a Hamiltonian that is constructed from the unperturbed densities:

$$(\mathcal{H}_0 + \mathcal{H}_{\mathrm{so}})[n_0, \mathbf{m}_0]\ \psi_{\mathrm{ft},\nu} = \epsilon_{\mathrm{ft},\nu}\ \psi_{\mathrm{ft},\nu}\ . \tag{9}$$

Thus, we have to determine the single-electron eigenvalues of the secular equation (9) only once.

Although our method allows for selfconsistent calculations of the unperturbed SSDWs, for small $\mathbf{q}$-vectors it is usually possible to treat the spiral boundary condition as well as the spin-orbit coupling as a perturbation. In this case, selfconsistent calculations have to be done only for $\mathbf{q} = 0$.

3.3. *First-order perturbation theory*

The easiest way to estimate the effect of the spin-orbit coupling operator $\mathcal{H}_{\mathrm{so}}$ on the band energies is first-order perturbation theory, i.e. the corrections to the band energies are approximated by the expectation values $\langle\psi_{0,\nu}|\mathcal{H}_{\mathrm{so}}|\psi_{0,\nu}\rangle$ of the spin-orbit operator and the unperturbed states $\psi_{0,\nu}$. These expectation values vanish for states with collinear magnetic order (and, therefore, give no contribution to the magnetocrystalline anisotropy), but they can be a good approximation for the antisymmetric exchange in noncollinear configurations.

The antisymmetric exchange interaction is expected to be largest in planar SSDWs, i.e. in spirals whose magnetization is confined to a plane normal to the rotation axis (cone angle $\vartheta = \frac{\pi}{2}$ in Eq. (3)) [5,6]. In such magnetic structures $\langle\psi_{0,\nu}|\mathcal{H}_{\mathrm{so}}|\psi_{0,\nu}\rangle$ describes only the odd part of the dispersion curve (2) and, therefore, the antisymmetric exchange interactions:

Assume, that the magnetization is confined to the (x,z)-plane, i.e. $m_y = 0$, which implies that $B_y = 0$ and $\mathcal{H}_0$ is real. In a crystal potential this real Hamiltonian has always two degenerate solutions, namely ψ and ψ^*. All components of the spin-orbit operator

$$\tilde{\mathcal{H}}_{\mathrm{so}} = \xi\,\sigma_x\,\ell_x + \xi\,\sigma_y\,\ell_y + \xi\,\sigma_z\,\ell_z = \sum_w \xi\,\sigma_w\,\ell_w \tag{10}$$

are Hermitian, which implies that $\langle\psi|\xi\,\sigma_w\,\ell_w|\psi\rangle$ is real. For $w \in \{x,z\}$, the operator $\xi\,\sigma_w\,\ell_w$ is purely imaginary and we obtain

$$\langle\psi^*|\xi\,\sigma_w\,\ell_w|\psi^*\rangle = -\langle\psi|\xi\,\sigma_w\,\ell_w|\psi\rangle^* = -\langle\psi|\xi\,\sigma_w\,\ell_w|\psi\rangle.$$

Thus, the expectation values of $\xi\,\sigma_x\,\ell_x$ and $\xi\,\sigma_z\,\ell_z$ cancel for each eigenspace of $\{\psi,\psi^*\}$ and we have to consider $\xi\,\sigma_y\,\ell_y$ only.

While this result was derived for $m_y = 0$, analogous relations hold for $m_z = 0$, too. This corresponds to a SSDW as described in Eq. (3) with $\vartheta = \frac{\pi}{2}$. Now, we will show that changing the sign of $\mathbf{q}$ also changes the sign of the matrix element $\langle\psi_{\mathbf{q}}|\xi\,\sigma_z\,\ell_z|\psi_{\mathbf{q}}\rangle$. Here, we exploit the fact that $\mathbf{q} \to -\mathbf{q}$ implies $m_y \to -m_y$, $B_y \to -B_y$, and $\mathcal{H}_0 \to \mathcal{H}_0^*$. If $\psi_{\mathbf{q}}$ is an eigenstate of $\mathcal{H}_0$ and can be described with Eq. (5), then $\psi_{\mathbf{q}}^* = \psi_{-\mathbf{q}}$ is a corresponding eigenstate of $\mathcal{H}_0^*$. Thus, we obtain

$$\langle\psi_{-\mathbf{q}}|\xi\,\sigma_z\,\ell_z|\psi_{-\mathbf{q}}\rangle = \langle\psi_{\mathbf{q}}|(\xi\,\sigma_z\,\ell_z)^*|\psi_{\mathbf{q}}\rangle^* =$$
$$-\langle\psi_{\mathbf{q}}|\xi\,\sigma_z\,\ell_z|\psi_{\mathbf{q}}\rangle^* = -\langle\psi_{\mathbf{q}}|\xi\,\sigma_z\,\ell_z|\psi_{\mathbf{q}}\rangle\ .$$

Note, that the first-order corrections to all bands can influence the sum of eigenvalues of occupied states. This is different for the higher-order corrections that determine the MCA, that depends mainly on the states in the vicinity of the Fermi energy. Therefore, the spin-orbit induced changes in the occupation numbers are less important for the antisymmetric exchange than for the magnetocrystalline anisotropy. The example in Section 4 illustrates that it is not necessary to recalculate the Fermi energy but sufficient to determine the occupied states before applying $\mathcal{H}_{\mathrm{so}}$ and to sum up the spin-orbit expectation values of these states.

3.4. *Diagonalization of the perturbed Hamiltonian*

If it is necessary to go beyond the previously discussed first-order perturbation and to solve the ac-

tual secular equation (9), an option is to expand the wavefunctions in the eigenfunctions of the unperturbed Hamiltonian $\mathcal{H}_0$. As these functions constitute a basis set that is well adopted for the studied problem, one needs relatively few basis functions (typically less than twice as many as occupied states) to describe the perturbed solution. This makes it feasible to set up and diagonalize a Hamiltonian matrix H including the matrix elements $\langle\psi_{0,\nu'}|\mathcal{H}_{\rm so}|\psi_{0,\nu}\rangle$ of the spin-orbit operator with the eigenfunctions $\{\psi_{0,\nu}\}$ of the unperturbed Hamiltonian $\mathcal{H}_0$. In the following we drop the index 0 and label the SSDW eigenfunctions of $\mathcal{H}_0$ as in Eq. (5) with their crystal momentum $\mathbf{k}$ and band index j, and we introduce the spin index σ. The matrix elements of these functions with the spin-orbit operator can be written as

$$\langle\psi_{\mathbf{k}',j'}|\mathcal{H}_{\rm so}|\psi_{\mathbf{k},j}\rangle = \sum_{\sigma',\sigma}\langle\psi^{(\sigma')}_{\mathbf{k}',j'}|\mathcal{H}^{(\sigma',\sigma)}_{\rm so}|\psi^{(\sigma)}_{\mathbf{k},j}\rangle\ . \tag{11}$$

When the (lattice periodic) operator $\mathcal{H}_{\rm so}$ acts on a Bloch function, it will leave the Bloch factor (including the $\pm\mathbf{q}/2$) unchanged, but transforms the lattice periodic part $u(\mathbf{r})$ to another lattice periodic function $\tilde{u}(\mathbf{r})$. Since a product of two lattice periodic functions can always be expanded in reciprocal lattice vectors of the (chemical) lattice, $\{\mathbf{G}\}$,

$$u_{\mathbf{k}',j'}(\mathbf{r})^*\,\tilde{u}_{\mathbf{k},j}(\mathbf{r}) = \sum_{\mathbf{G}} c_{\mathbf{G}}\,e^{i\,\mathbf{G}\cdot\mathbf{r}}\,, \tag{12}$$

we can write the matrix elements as

$$\begin{aligned}&\int \mathrm{d}\mathbf{r}\ (e^{i\,(\mathbf{k}'+\frac{\mathbf{q}'}{2})\cdot\mathbf{r}}u_{\mathbf{k}',j'})^*\,(e^{i\,(\mathbf{k}+\frac{\mathbf{q}}{2})\cdot\mathbf{r}}\tilde{u}_{\mathbf{k},j}) \\ &\quad=\sum_{\mathbf{G}} c_{\mathbf{G}}\int\mathrm{d}\mathbf{r}\,e^{i(\mathbf{G}+\mathbf{k}-\mathbf{k}'+\frac{\mathbf{q}}{2}-\frac{\mathbf{q}'}{2})\cdot\mathbf{r}}\end{aligned} \tag{13}$$

with $\mathbf{q}'=\pm\mathbf{q}$. Considering that $\lim_{R\to\infty}\ \frac{1}{R}\int_0^R\mathrm{d}r\ e^{i\,x\,r}$ vanishes for any $x\neq 0$, we obtain

$$\begin{aligned}
&\langle\psi^{(\uparrow)}_{\mathbf{k}',j'}|\mathcal{H}^{(\uparrow,\uparrow)}_{\rm so}|\psi^{(\uparrow)}_{\mathbf{k},j}\rangle\neq 0\ \ \Rightarrow\ \ \mathbf{k}-\mathbf{k}'\in\{\mathbf{G}\}\ ,\\
&\langle\psi^{(\uparrow)}_{\mathbf{k}',j'}|\mathcal{H}^{(\uparrow,\downarrow)}_{\rm so}|\psi^{(\downarrow)}_{\mathbf{k},j}\rangle\neq 0\ \ \Rightarrow\ \ \mathbf{k}-\mathbf{k}'+\mathbf{q}\in\{\mathbf{G}\}\ ,\\
&\langle\psi^{(\downarrow)}_{\mathbf{k}',j'}|\mathcal{H}^{(\downarrow,\uparrow)}_{\rm so}|\psi^{(\uparrow)}_{\mathbf{k},j}\rangle\neq 0\ \ \Rightarrow\ \ \mathbf{k}-\mathbf{k}'-\mathbf{q}\in\{\mathbf{G}\}\ ,\\
&\langle\psi^{(\downarrow)}_{\mathbf{k}',j'}|\mathcal{H}^{(\downarrow,\downarrow)}_{\rm so}|\psi^{(\downarrow)}_{\mathbf{k},j}\rangle\neq 0\ \ \Rightarrow\ \ \mathbf{k}-\mathbf{k}'\in\{\mathbf{G}\}\ .
\end{aligned} \tag{14}$$

According to Eq. (14), the Hamiltonian matrix is not block diagonal in $\mathbf{k}$, but there are non-vanishing matrix elements between states whose $\mathbf{k}$-vectors are connected by $\mathbf{q}$. If the $\mathbf{q}$-vector is a fraction of a reciprocal lattice vector $\mathbf{G}$ (i.e. $\mathbf{q}=\frac{1}{n}\mathbf{G}$, n integer) then the Hamiltonian matrix can be partitioned in blocks of the form as indicated in Fig. 1. The size of the submatrices (named A_i and B_i in Fig. 1) depends on the number of basis functions (i.e. unperturbed states) that are

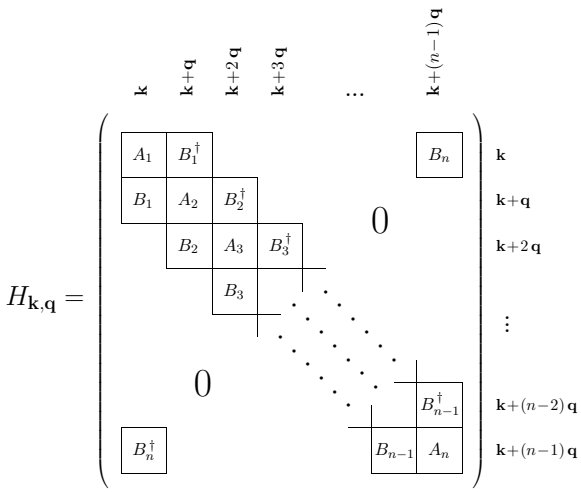

Fig. 1. Block of the Hamiltonian matrix $H=\delta_{\nu,\nu'}\,\epsilon_{0,\nu}+H_{\rm so}$ for a the $\mathbf{k}$-point set $\{\mathbf{k},\mathbf{k}+\mathbf{q},\ldots\}$. Only the submatrices marked with B mix between spin-↑ and spin-↓. For large n, most matrix elements are zero.

used to expand the eigenfunctions of the full Hamiltonian $\mathcal{H}_0+\mathcal{H}_{\rm so}$. The number of these submatrices depends on the $\mathbf{q}$-vector: n corresponds to the number of chemical unit cells that are required to fill a magnetic unit cell that is commensurate with the chemical lattice. Thus, $\mathbf{q}$ cannot be chosen arbitrarily. The optimal ratio of matrix size to spiral period length is achieved for $\mathbf{q}=\frac{1}{n}\hat{\mathbf{G}}$ with integer n and a primitive reciprocal lattice vector $\hat{\mathbf{G}}$. In this case, one spiral period is a multiple of the chemical lattice and the size of the matrix block shown in Fig. 1 is proportional to the spiral period length. Note, that the reciprocal unit cell of the chemical lattice is n times larger than the reciprocal unit cell of the commensurate magnetic lattice and the n different $\mathbf{k}$-vectors which contribute to the block matrix in Fig. 1 correspond to only one point in the reciprocal magnetic unit cell.

In order to compare the energies of different magnetic configurations, one should calculate all these energies with the same $\mathbf{k}$-point set. Thus, to determine the $\mathbf{q}$-dependent spin-orbit corrections to the SSDW energies (and hence D) special care has to be taken to choose the $\mathbf{k}$- and $\mathbf{q}$-grid accordingly in order to allow for the calculation of the matrix elements (14).

In the case of large spiral periods the Hamiltonian matrix H gets very large and it is not always feasible to diagonalize it exactly. Fortunately, one does not need the entire spectrum but the sum of eigenvalues of the occupied states (cf. Eq. (8)). In Appendix A we present a method to approximate this sum without diagonalizing the full matrix. When this method is applied, most computational resources are needed to determine the eigenstates $\{\psi_{\mathbf{k},j}\}$ of the unperturbed Hamiltonian $\mathcal{H}_0$, as this has to be done for many $\mathbf{k}$-vectors. Here, we ex-

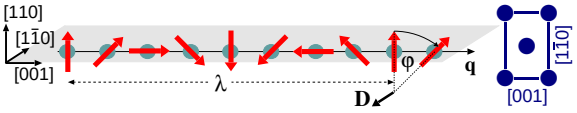

Fig. 2. Schematic drawing of the magnetization profile of the calculated SSDWs. In the right figure, the orientation of the conventional surface unit cell is indicated.

pect some improvement from an interpolation scheme like the one described in Ref. [15].

In the case of small **q**-vectors and accordingly large n, the sparseness of the Hamiltonian matrix H considerably reduces the number of matrix elements to be calculated and stored in the computer memory.

4. Example: Fe/W(110) and Fe/Mo(110)

To demonstrate the power of the outlined approach, we investigate here two model systems: a Fe-monolayer deposited on the W(110) and Mo(110)-surface, respectively. While W and Mo are chemically and structurally very similar, the spin-orbit coupling strength (ξ in Eq. (6)) is much larger in W than in Mo. In our calculations only three layers of W (Mo) are used as substrate, which might be too few for a realistic simulation but sufficient for our analysis. To suppress the effects of the artificially introduced substrate-vacuum interface (opposite to the Fe-layer), we exclude the spin-orbit effects in this substrate-layer from the Hamiltonian.

The calculated magnetic configurations are homogeneous SSDWs with the **q**-vectors pointing in [001]-direction (remember, that **q** determines the propagation direction, the period length and the rotational direction, Fig. 2). In this geometry, we expect the highest contribution to the Dzyaloshinskii-Moriya interaction for SSDWs with a spin rotation axis along [1$\bar{1}$0] (normal to the propagation direction) and a magnetization confined to the plane normal to [1$\bar{1}$0] (cone angle $\vartheta = \frac{\pi}{2}$ in Eq. (3)).

We employ the local density approximation and the full-potential linearized augmented planewave method as implemented in the FLEUR code [16,17].

	Fe/W(110)	Fe/Mo(110)
matrix diag.:	$D^{@W}_{diag} = -7.8\,\frac{meV}{nm}$	$D^{@Mo}_{diag} = -1.2\,\frac{meV}{nm}$
1st-order pert.:		
Fe-layer	$D^{@W}_{Fe} = 3.6\,\frac{meV}{nm}$	$D^{@Mo}_{Fe} = 4.0\,\frac{meV}{nm}$
1st sub. layer	$D^{@W}_{W1} = -10.9\,\frac{meV}{nm}$	$D^{@Mo}_{Mo1} = -4.6\,\frac{meV}{nm}$
Fe + 2 sub.layers	$D^{@W}_{pert} = -10.2\,\frac{meV}{nm}$	$D^{@Mo}_{pert} = -1.4\,\frac{meV}{nm}$

Table 1
Dzyaloshinskii parameters obtained by linear fits to the data shown in Fig. 3. In the case of the first-order perturbation, the occupation numbers are determined for the unperturbed system only (fix occ. in the left panel of Fig. 3).

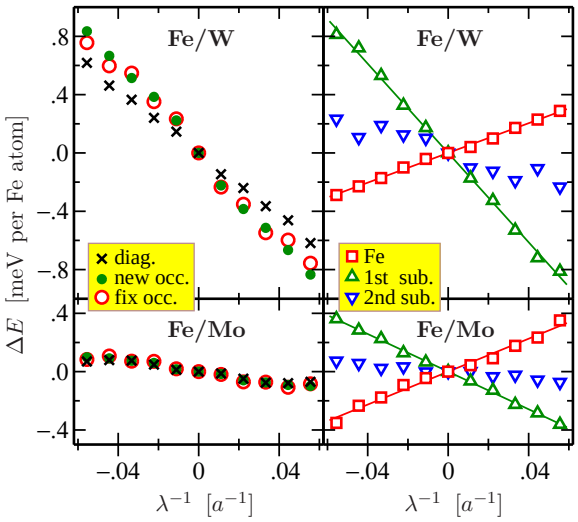

Fig. 3. Spin-orbit induced corrections to the SSDW energy. The data in the upper (lower) panel is obtained for a Fe-monolayer deposited on three W- (Mo-)layers, details of the setup are given in the text. The spiral period $|\lambda| = \frac{2\pi}{|\mathbf{q}|}$ is given with respect to the substrate lattice constant a, for $\mathbf{q} \| [001]$ the antiferromagnetic configuration corresponds to $|\lambda| = a$. Left panels: The odd part of the dispersion $E(\lambda^{-1})$ obtained by matrix diagonalization, cf. Section 3.4 (diag.); the sum of eigenvalues obtained by accounting for the first-order corrections to the band energies and the resulting changes in the Fermi energy and occupation numbers (new occ.); the sum of first-order corrections to the occupied states of the unperturbed SSDWs (fix occ.). Right panels: Contribution of the Fe and 1st and 2nd substrate layer to the corrections to the occupied states of the unperturbed SSDWs. The solid lines represent linear fits to the DFT data.

We use a planewave cutoff of 7 Å^{-1} and the muffin-tin radii 1.11 Å (Fe) and 1.32 Å (substrate). The potential is calculated selfconsistently for the ferromagnetic configuration with 484 $\mathbf{k}_\parallel$-points and the perturbative scheme is carried out with 3780 $\mathbf{k}_\parallel$-points in the two-dimensional Brillouin zone that corresponds to the chemical unit cell. The SOC Hamiltonian is constructed from 108 SSDW states per submatrix A_i (cf. Fig. 1). It is diagonalized in the interval given by $e_0 = 2.7$ eV (cf. Appendix A). The resulting values for ΔE differ for Fe/W(110) by 4 μeV from ΔE obtained by diagonalizing the full Hamiltonian for $|a/\lambda| \geq 0.022$. The lattice constants are $a_W = 3.16$ Å and $a_{Mo} = 3.16$ Å, the surface relaxations are $d_{Fe-W} = 1.92$ Å and $d_{Fe-Mo} = 1.94$ Å.

The results are shown in Fig. 3. Here, we consider only the odd part of the dispersion curves $E(\lambda^{-1})$ for large λ. The slopes of these curves correspond to D in the micromagnetic model (1). In the left panels of the figure, we compare the different perturbative approaches: it can be seen that the contributions beyond first-order perturbation theory are rather small. Also changes in the occupation numbers are of minor im-

portance.

In the right panels, we compare the contributions of the different atoms. This analysis is done for first-order perturbation theory only, and in Eq. (6) only the terms belonging to the selected atom are taken into account. The linear fits to the *ab initio* data are summarized in Table 1. Note, that the atom-resolved spin-orbit matrix elements of atoms with equivalent valence band configurations increase rapidly with the atomic number Z [12]. The Dzyaloshinskii parameter depends linearly and the MCA depends quadratically on these matrix elements. We obtain $D_{\mathrm{Fe}}^{@\mathrm{W}}/D_{\mathrm{Fe}}^{@\mathrm{Mo}} = 0.9$ and $D_{\mathrm{W1}}^{@\mathrm{W}}/D_{\mathrm{Mo1}}^{@\mathrm{Mo}} = 2.4$ (with $Z_{\mathrm{W}} = 74$ and $Z_{\mathrm{Mo}} = 42$, and a radially averaged ratio $\bar{\xi}_{\mathrm{W}}/\bar{\xi}_{\mathrm{Mo}} = 3.6$ in Ref. [12]). In the W-case, the substrate gives a larger contribution to D than the Fe-layer although the corresponding magnetic moments are $0.1\,\mu_{\mathrm{B}}$ (1st W) and $2.3\,\mu_{\mathrm{B}}$ (Fe). In the Mo-case, the contribution of the substrate is almost compensated by the Fe-contribution and the magnetic moments are $0.1\,\mu_{\mathrm{B}}$ (1st Mo) and $2.4\,\mu_{\mathrm{B}}$ (Fe).

5. Summary

We presented a computationally efficient method to determine the strength of the DM-interaction from the spin-orbit induced corrections to the energy of long-ranged spin spirals. Our calculations show that the inclusion of SOC by first-order perturbation theory is reasonably accurate. Application of our method in the investigation of realistic magnetic nanostructures can provide deeper understanding of the role of antisymmetric exchange interactions that remained rather unexplored up to now.

Appendix A. Perturbative approach for the sum of eigenvalues

Here, we present a method that allows to estimate the changes of the sum of eigenvalues of the occupied states (due to the perturbation $\mathcal{H}_{\mathrm{so}}$) beyond first-order perturbation theory. The ordinary second-order Raleigh-Schrödinger perturbation theory very accurately describes the energy corrections due to the interactions of states that are well (more than e_Δ) separated in energy, but is not feasible if the interacting states are close in energy. Since we are interested only in the sum of eigenvalues of the occupied states, we can diagonalize a (relatively small) Hamiltonian submatrix $\mathcal{H}_1$ that mixes only among the states in the vicinity of the Fermi level ϵ_{F}, and treat the remaining interactions between occupied and unoccupied states in second-order perturbation theory. The effects due

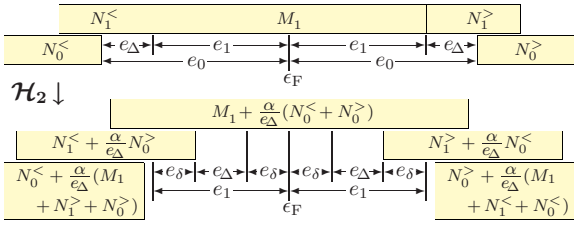

Fig. A.1. Sketch illustrating the defined energies and sets. The upper part represents the eigenfunctions of $(\mathcal{H}_0 + \mathcal{H}_1)$, the lower part the changes obtained when applying $\mathcal{H}_2$. The horizontal axis represents the energy intervals. $M_1 + \frac{\alpha}{e_\Delta}(N_0^< + N_0^>)$ denotes states of the form $|\psi_a\rangle + \sum_b c_b |\psi_b\rangle$, with $|\psi_a\rangle \in M_1$, $|\psi_b\rangle \in (N_0^< \cup N_0^>)$, and $|c_b| < \alpha/e_\Delta$. $\mathcal{H}_2$ does not mix among states that are closer in energy than e_Δ.

to the interactions among states, that are low enough in energy to remain entirely occupied, mutually cancel and have no effect on the eigenvalue sum.

Let us introduce a quantity α so that $|\langle\psi'|\mathcal{H}_{\mathrm{so}}|\psi\rangle| < \alpha$ for all states ψ', ψ. We develop a perturbative expansion, where terms of the order α^3/e_Δ^2 are truncated. Thereby, the energy difference e_Δ determines the accuracy of our treatment. Further, we introduce the energy e_δ: If any Hamiltonian with a spectrum confined in the interval $[\epsilon_{\min}, \epsilon_{\max}]$ is perturbed by SOC, we assume that the spectrum of the resulting perturbed Hamiltonian is confined in $[\epsilon_{\min} - e_\delta, \epsilon_{\max} + e_\delta]$.

The Schrödinger-type Hamiltonian (4) and its eigenstates and eigenvalues are denoted with $\mathcal{H}_0$, $\psi_{0,\nu}$ and $\epsilon_{0,\nu}$, respectively. At first, we divide the set $\{\psi_{0,\nu}\}$ in states with eigenvalues $\epsilon_{0,\nu}$ close to, well below, and well above the Fermi level ϵ_{F}:

$$M_0 = \{\psi_{0,\nu} \;\big|\; |\epsilon_{0,\nu} - \epsilon_{\mathrm{F}}| \le e_0\}\,,$$
$$N_0^< = \{\psi_{0,\nu} \;\big|\; \epsilon_{0,\nu} < \epsilon_{\mathrm{F}} - e_0\}\,,$$
$$N_0^> = \{\psi_{0,\nu} \;\big|\; \epsilon_{0,\nu} > \epsilon_{\mathrm{F}} + e_0\}\,.$$

We introduce the notation

$$\mathcal{H}(X,Y) = \sum_{\psi' \in X\,,\,\psi \in Y} |\psi'\rangle\langle\psi'|\mathcal{H}_{\mathrm{so}}|\psi\rangle\langle\psi| + h.c.$$

and define $\mathcal{H}_1 = \mathcal{H}(M_0, M_0)$. For sufficiently small e_0, $(\mathcal{H}_0 + \mathcal{H}_1)$ can be treated by exact diagonalization. Its eigenstates and eigenvalues are denoted with $\psi_{1,\nu}$ and $\epsilon_{1,\nu}$. In order to treat $(\mathcal{H}_{\mathrm{so}} - \mathcal{H}_1)$, we choose e_1 (with $2\,e_\delta + e_\Delta < e_1 < e_0 - e_\Delta$) and split span M_0 (i.e. the linear combinations of the elements of M_0) according to the eigenvalues $\{\epsilon_{1,\nu}\}$ of $(\mathcal{H}_0 + \mathcal{H}_1)$:

$$M_1 = \{\psi_{1,\nu} \in \mathrm{span}\, M_0 \;\big|\; |\epsilon_{1,\nu} - \epsilon_{\mathrm{F}}| \le e_1\}\,,$$
$$N_1^< = \{\psi_{1,\nu} \in \mathrm{span}\, M_0 \;\big|\; \epsilon_{1,\nu} < \epsilon_{\mathrm{F}} - e_1\}\,,$$
$$N_1^> = \{\psi_{1,\nu} \in \mathrm{span}\, M_0 \;\big|\; \epsilon_{1,\nu} > \epsilon_{\mathrm{F}} + e_1\}$$

(cf. Fig. A.1). With these sets, we define

$$\begin{aligned}\mathcal{H}_2 = \quad & \mathcal{H}(N_0^<, N_1^>) + \mathcal{H}(N_0^<, M_1) \\ & + \mathcal{H}(N_0^>, N_1^<) + \mathcal{H}(N_0^>, M_1) + \mathcal{H}(N_0^<, N_0^>) \ , \\ \mathcal{H}_3 = \quad & \mathcal{H}(N_0^<, N_0^<) + \mathcal{H}(N_0^>, N_0^>) \\ & + \mathcal{H}(N_0^<, N_1^<) + \mathcal{H}(N_0^>, N_1^>) \ .\end{aligned}$$

Noting that $\psi_{0,\nu} \notin M_0$ implies $\psi_{0,\nu} = \psi_{1,\nu}$, we obtain for the remaining perturbation

$$\begin{aligned}\mathcal{H}_{\rm so} - \mathcal{H}_1 &= \mathcal{H}(N_0^<, M_0) + \mathcal{H}(N_0^>, M_0) + \mathcal{H}(N_0^<, N_0^>) \\ &\quad + \mathcal{H}(N_0^<, N_0^<) + \mathcal{H}(N_0^>, N_0^>) \\ &= \mathcal{H}_2 + \mathcal{H}_3 \ .\end{aligned}$$

The corrections to $\{\epsilon_{1,\nu}\}$ due to $\mathcal{H}_2$ can be estimated in 2nd-order perturbation theory, as all energy denominators are larger than $\min\{2\,e_1\,,\ e_0 - e_1\} > e_\Delta$:

$$\begin{aligned}\epsilon_{2,\nu} = \quad & \epsilon_{1,\nu} + \langle\psi_{1,\nu}|\mathcal{H}_2|\psi_{1,\nu}\rangle \\ & + \sum_{\nu'} \frac{|\langle\psi_{1,\nu'}|\mathcal{H}_2|\psi_{1,\nu}\rangle|^2}{\epsilon_\nu - \epsilon_{\nu'}} \ .\end{aligned} \tag{A.1}$$

Hereby, the numerical effort is reduced by exploiting the sparseness of $\mathcal{H}_{\rm so}$. The corrections to the states $\{\psi_{1,\nu}\}$ due to $\mathcal{H}_2$ are of the order α/e_Δ, the corrected states are

$$|\psi_{2,\nu}\rangle = |\psi_{1,\nu}\rangle + \sum_{\nu'} |\psi_{1,\nu'}\rangle \frac{\langle\psi_{1,\nu'}|\mathcal{H}_2|\psi_{1,\nu}\rangle}{\epsilon_{1,\nu} - \epsilon_{1,\nu'}} + \mathcal{O}(\tfrac{\alpha^2}{e_\Delta^2}) \, .$$

In the next step, we define

$$\mathcal{H}_3^< = \sum_{\psi',\psi \in N_2^<} |\psi'\rangle\langle\psi'|\mathcal{H}_3|\psi\rangle\langle\psi| + h.c.$$

with $N_2^< = \{\psi_{2,\nu} \ \big| \ \epsilon_{2,\nu} < \epsilon_{\rm F} - e_\delta\}$, and an equivalent nomenclature for ">". If neither ($\psi_{1,\nu} \in N_0^< \cup N_1^<$ and $\psi_{1,\nu'} \in N_0^< \cup N_1^<$) nor ($\psi_{1,\nu} \in N_0^> \cup N_1^>$ and $\psi_{1,\nu'} \in N_0^> \cup N_1^>$), then $\langle\psi_{2,\nu'}|\mathcal{H}_3|\psi_{2,\nu}\rangle$ is of the order α^2/e_Δ . Due to our choice $e_1 > 2\,e_\delta + e_\Delta$, either $\langle\psi_{2,\nu'}|\mathcal{H}_3 - \mathcal{H}_3^> - \mathcal{H}_3^<|\psi_{2,\nu}\rangle$ is of the order α^3/e_Δ^2 or $|\epsilon_{2,\nu'} - \epsilon_{2,\nu}| > e_\Delta$ (cf. Fig. A.1). Therefore, a matrix element of $(\mathcal{H}_3 - \mathcal{H}_3^> - \mathcal{H}_3^<)$ can either be neglected in the Hamiltonian or its effect on the eigenvalue spectrum (Eq. (A.1)) can be neglected.

We still have to account for the perturbation $(\mathcal{H}_3^> + \mathcal{H}_3^<)$ on the energies $\{\epsilon_{2,\nu}\}$. The operator $\mathcal{H}_3^>$ mixes only among unoccupied states, whose energies are higher than $\epsilon_{\rm F} + e_\delta$. According to our definition of e_δ , these states remain unoccupied when their energies are perturbed by $\mathcal{H}_3^>$. Their energies do not influence the sum of energies of occupied states. The operator $\mathcal{H}_3^<$ mixes only among occupied states, whose energies are lower than $\epsilon_{\rm F} - e_\delta$. According to our definition of e_δ , these states remain occupied when their energies are perturbed by $\mathcal{H}_3^<$. The influence of $\mathcal{H}_3^<$ on the sum of energies of occupied states is given by the trace of the perturbation:

$$\mathrm{tr}\langle\psi_{2,\nu'}|\mathcal{H}_3^<|\psi_{2,\nu}\rangle_{\nu,\nu'} = \sum_{\psi \in N_0^<} \langle\psi|\mathcal{H}_{\rm so}|\psi\rangle + \mathcal{O}(\tfrac{\alpha^3}{e_\Delta^2}) \, . \tag{A.2}$$

Thus, we have to choose e_0, diagonalize $(\mathcal{H}_0 + \mathcal{H}_1)$, choose e_1 (e.g. half the value of e_0), evaluate Eq. (A.1), update $e_{\rm F}$ and evaluate the sum in Eq. (A.2).

We acknowledge financial support from the Deutsche Forschungsgemeinschaft (Grant No. BI823/1-1) and from the ESF EUROCORES Programme SONS (Contract No. ERAS-CT-2003-980409).

References

[1] C. Herring, *Exchange interactions among itinerant electrons, Magnetism Vol. IV*, ed. G. T. Rado, H. Suhl, Academic Press, New York, London, 1966.

[2] L. M. Sandratskii, J. Phys.: Cond. Matter **3**, 8565 (1991).

[3] M. Bode, M. Heide, K. von Bergmann, P. Ferriani, S. Heinze, G. Bihlmayer, A. Kubetzka, O. Pietzsch, S. Blügel, and R. Wiesendanger, Nature (London) **447**, 190 (2007).

[4] P. Ferriani, K. von Bergmann, E. Y. Vedmedenko, S. Heinze, M. Bode, M. Heide, G. Bihlmayer, S. Blügel, and R. Wiesendanger, Phys. Rev. Lett. **101**, 027201 (2008).

[5] I. E. Dzyaloshinskiĭ, Sov. Phys. JETP **20**, 665 (1965).

[6] Y. A. Izyumov, Sov. Phys. Usp. **27**, 845 (1984).

[7] T. Moriya, Phys. Rev. **120**, 91 (1960).

[8] M. Heide, G. Bihlmayer, and S. Blügel, Phys. Rev. B **78**, 140403(R) (2008).

[9] D. D. Koelling and B. N. Harmon, J. Phys. C: Solid State Phys. **10**, 3107 (1977).

[10] A. H. MacDonald, W. E. Pickett, and D. D. Koelling, J. Phys. C: Solid State Phys. **13**, 2675 (1980).

[11] ξ depends on the spin-dependent gradient of the potential and on the angular momentum ℓ. The ℓ-dependence is accounted for in the actual calculation, but dropped here to simplify the discussion. The spin-dependence is neglected in the calculation, as our method relies on a lattice-periodic spin-orbit operator. This does not present a problem, as ξ is dominated by the large gradient of the Coulomb potential in the vicinity of the nuclei.

[12] A. R. Mackintosh and O. K. Andersen, *Electrons at the Fermi Surface*, p. 149, ed. M. Springford, Cambridge Univ. Press, London, 1980.

[13] A. Oswald, R. Zeller, P. J. Braspenning, and P. H. Dederichs, J. Phys. F: Met. Phys. **15**, 193 (1985).

[14] A. I. Liechtenstein, M. I. Katsnelson, V. P. Antropov, and V. A. Gubanov, J. Magn. Magn. Mater. **67**, 65 (1987).

[15] J. R. Yates, X. Wang, D. Vanderbilt, and I. Souza, Phys. Rev. B **75**, 195121 (2007).

[16] P. Kurz, F. Förster, L. Nordström, G. Bihlmayer, and S. Blügel, Phys. Rev. B **69**, 024415 (2004).

[17] For a program description see *http://www.flapw.de* .